Proceedings of the ASME 2013 International Design Engineering Technical Conferences & Conference on Mechanical Vibration and Noise
IDETC/VIB 2013
August 04-07, 2013, Portland, OR, USA

DETC2013-13207: DRAFT

SECOND-ORDER PERTURBATION ANALYSIS OF LOW-AMPLITUDE TRAVELING WAVES IN A PERIODIC NONLINEAR CHAIN

Smruti R. Panigrahi*
Dynamics and Vibrations
Research Laboratory
Dept. of Mechanical Engineering
Michigan State University
E. Lansing, Michigan, 48824
Email: smruti@msu.edu
Phone: 517-515-1620

Brian F. Feeny
Dept. of Mechanical Engineering
Michigan State University
E. Lansing, Michigan, 48824
Email: feeny@egr.msu.edu
Phone: 517-353-9451
Fax: 517-353-1750

Alejandro R. Diaz
Dept. of Mechanical Engineering
Michigan State University
E. Lansing, Michigan, 48824
Email: diaz@egr.msu.edu
Phone: 517-353-9861
Fax: 517-353-1750

ABSTRACT

Traveling waves in one-dimensional nonlinear periodic structures are investigated for low-amplitude oscillations using perturbation analysis. We use second-order multiple scales analysis to capture the effect of quadratic nonlinearity. Comparisons with the linear and cubical nonlinear cases are presented in the dispersion relationship, group velocity and phase velocity and their dependence on wave number and amplitude of oscillation. Quadratic nonlinearity is shown to have a significant effect on the behavior.

Keywords: Traveling waves, nonlinear periodic structures, second-order perturbation, method of multiple scales, amplitude-dependent dispersion, nonlinear waveguides, metamaterials, acoustic filters

1 Introduction

Metamaterials have been of growing interest for achieving certain desirable properties such as band gaps, negative refractive indices, phonon tunneling, and phonon focusing [1]. Engineering applications of these properties are in waveguides, acoustic filters, acoustic mirrors, transducers, etc. [2–8]. Various types of periodic media have been studied, including one-dimensional undamped mass-spring chains [9–12], strongly nonlinear contact in beaded systems [13], kink dynamics [14], and weakly coupled layered systems [15, 16].

Due to the presence of band gaps in periodic media, many researchers have been focusing on wave propagation in nonlinear periodic structures and its application to the design of novel metamaterials [3, 9–11, 17–20]. Structures exhibiting bandgaps prevent the propagation of waves at certain frequencies. These structures may be phononic (sonic) or photonic, depending on their band-gap frequency range. Phononic or sonic band-gap structures can be used as sensing devices based on resonators, acoustic logic ports and wave guides, and frequency filters based on surface acoustic waves, while photonic band-gap structures have applications in optics and microwaves. Synthesis of phononic materials with desired band-gap and wave-guiding characteristics has been achieved through the application of topology and material optimization procedures [7, 21, 22]. The application of periodic plane grid structures as phononic materials and its design optimization process has been presented in [23], where a limited number of continuously varying parameters define the geometry of a predefined cellular topology that deals with periodic structures of infinite size as well as demonstrate the validity of the results to finite systems.

Amplitude-dependent dispersion and band-gap behavior have been explored in several discrete periodic systems characterized by cubic nonlinearities by Narisetti et al. [10], where it was shown that the boundary of the dispersion curve may shift with amplitude in the presence of a single plane wave. Manktelow et al. [24] have recently extended the analysis in [10] to include the propagation of multiple harmonic plane waves that show the

*Address all correspondence to this author.

dispersion properties of discrete, periodic, cubically nonlinear systems. They presented a comparison between the multiple scales and Lindstedt-Poincare method for harmonic wave-wave interactions due to commensurate frequency ratios. Narisetti et al. [11] have recently studied a plane wave propagation in strongly nonlinear periodic media. At higher frequencies and low amplitudes, it is shown that a hexagonally-packed and prestressed lattice exhibits acoustic wave beaming phenomena and may have applications in tunable spatial filters and tunable stress-redirecting materials.

While these studies address cubic nonlinear periodic media for applications as metamaterials, there has been no research on wave propagations in periodic media with strong quadratic nonlinearities. We look at small amplitude waves propagating about an equilibrium configuration of a snap-through periodic chain, and retain quadratic and cubic nonlinearity local to the equilibrium. A second-order multiple scales perturbation analysis is applied for low-amplitude oscillations that capture the quadratic effects. We obtain a nonlinear dispersion relationship from the theoretical analysis and compare it to linear and cubically nonlinear cases. The amplitude dependence of the dispersion relations shows that the mass-spring chains can be used as tunable acoustic filters. The group and phase velocity dependence on wave number and amplitude shows the relevance of quadratic effects for applications in band gaps, event detection and nonlinear waveguides.

2 Periodic Chain of Snap-Through Oscillators

We study the wave behaviors in an infinite uniform nonlinear mass-spring chain (Figure 1). Due to the snap-through behavior of the individual elements (Figure 2), it is suspected that there will be a nonlinear wave phenomenon for an infinite element system.

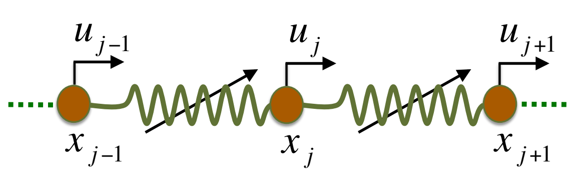

FIGURE 1: Infinite mass chain. The unstretched position and displacement of mass m_j are denoted by x_j and u_j respectively. The springs are cubic nonlinear as in Figure 2 with unstretched length h.

The mass-spring chain is arranged in a fashion such that each mass is separated by a distance h from its nearest neighbor. h is also the un-stretched length of each spring before any snap-through occurs. We use the assumption that all the masses are equal ($m_j = m$) and only the nearest neighbors have direct effects on each other. The equations of motion (EOM) can then be written as

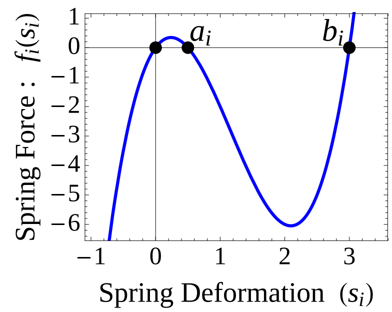

FIGURE 2: The characteristic spring force $f_i(s_i)$ of the nonlinear spring as a function of the spring deformation s_i.

$$\begin{aligned} m\ddot{u}_j = & \quad \tilde{\alpha}\left[(u_{j+1}-u_j)-(u_j-u_{j-1})\right] \\ & + \quad \tilde{\beta}\left[(u_{j+1}-u_j)^2-(u_j-u_{j-1})^2\right] \\ & + \quad \tilde{\gamma}\left[(u_{j+1}-u_j)^3-(u_j-u_{j-1})^3\right] \end{aligned} \tag{1}$$

for $j = \cdots, -2, -1, 0, 1, 2, \cdots$. To simplify the equation we apply the following coordinate transformation:

$$\varepsilon\, z_j = \left(u_{j+1}-u_j\right) \tag{2}$$

Letting $\alpha = \frac{\tilde{\alpha}}{m}$, $\beta = \frac{\tilde{\beta}}{m}$, $\gamma = \frac{\tilde{\gamma}}{m}$, the equations become

$$\ddot{u}_{j+1} = \varepsilon\,\alpha\left(z_{j+1}-z_j\right)+\varepsilon^2\,\beta\left(z_{j+1}^2-z_j^2\right)+\varepsilon^3\,\gamma\left(z_{j+1}^3-z_j^3\right) \tag{3}$$

$$\ddot{u}_j = \varepsilon\,\alpha\left(z_j-z_{j-1}\right)+\varepsilon^2\,\beta\left(z_j^2-z_{j-1}^2\right)+\varepsilon^3\,\gamma\left(z_j^3-z_{j-1}^3\right) \tag{4}$$

Now subtracting equation (4) from equation (3), we obtain the equation of motion in the z coordinates

$$\begin{aligned} \ddot{z}_j = -\alpha\left(2\,z_j-z_{j+1}-z_{j-1}\right)-\varepsilon\,\beta\left(2\,z_j^2-z_{j+1}^2-z_{j-1}^2\right) \\ -\varepsilon^2\,\gamma\left(2\,z_j^3-z_{j+1}^3-z_{j-1}^3\right) \end{aligned} \tag{5}$$

When ε is small, we are considering the spring deformation near one of the stable equilibria, i.e. it does not snap through. With ε as a bookkeeping parameter, the quadratic effect is more dominant than the cubic in equation (5). With the small parameter ε, we will analyze these ordinary differential equations by using the method of multiple scales next.

3 Second-Order Multiple Scales Analysis

3.1 Analysis in Strain Coordinates

We analyze the wave equation using the method of multiple scales (MMS). We assume,

$$
\begin{aligned}
&z_j(t) = z_{j_0}(T_0,T_1,T_2) + \varepsilon\, z_{j_1}(T_0,T_1,T_2) + \varepsilon^2\, z_{j_2}(T_0,T_1,T_2) + \cdots \\
&\frac{d}{dt} = D_0 + \varepsilon D_1 + \varepsilon^2 D_2 + \cdots \\
&\frac{d^2}{dt} = D_0^2 + \varepsilon\,(2D_0D_1) + \varepsilon^2\left(D_1^2 + 2D_0D_2\right) + \cdots
\end{aligned}
\tag{6}
$$

where $D_i = \frac{\partial}{\partial T_i}$. Plugging into equation (5) yields

$$
\begin{aligned}
&D_0^2 z_{j_0} + \varepsilon\left[D_0^2 z_{j_1} + 2D_0D_1 z_{j_0}\right] + \varepsilon^2\left[D_0^2 z_{j_2} + 2D_0D_1 z_{j_1}\right.\\
&\left. + \left(D_1^2 + 2D_0D_2\right) z_{j_0}\right] = -\alpha\left[2\, z_{j_0} - z_{j+1_0} - z_{j-1_0}\right]\\
&-\varepsilon\left[\alpha\left(2\, z_{j_1} - z_{j+1_1} - z_{j-1_1}\right) + \beta\left(2\, z_{j_0}^2 - z_{j+1_0}^2 - z_{j-1_0}^2\right)\right]\\
&-\varepsilon^2\left[\alpha\left(2\, z_{j_2} - z_{j+1_2} - z_{j-1_2}\right) + \gamma\left(2\, z_{j_0}^3 - z_{j+1_0}^3 - z_{j-1_0}^3\right)\right.\\
&\left. + 2\,\beta\left(2\, z_{j_0} z_{j_1} - z_{j+1_0} z_{j+1_1} - z_{j-1_0} z_{j-1_1}\right)\right]
\end{aligned}
\tag{7}
$$

Equating like powers of ε,

$$
\varepsilon^0 : D_0^2 z_{j_0} + \alpha\left(2\, z_{j_0} - z_{j+1_0} - z_{j-1_0}\right) = 0 \tag{8}
$$

$$
\begin{aligned}
\varepsilon^1 :\ & D_0^2 z_{j_1} + \alpha\left(2\, z_{j_1} - z_{j+1_1} - z_{j-1_1}\right) = \\
& -2D_0D_1 z_{j_0} - \beta\left(2\, z_{j_0}^2 - z_{j+1_0}^2 - z_{j-1_0}^2\right)
\end{aligned}
\tag{9}
$$

$$
\begin{aligned}
\varepsilon^2 :\ & D_0^2 z_{j_2} + \alpha\left(2\, z_{j_2} - z_{j+1_2} - z_{j-1_2}\right) = \\
& -2D_0D_1 z_{j_1} - \left(D_1^2 + 2D_0D_2\right) z_{j_0} \\
& -\beta\left(2\, z_{j_0} z_{j_1} - z_{j+1_0} z_{j+1_1} - z_{j-1_0} z_{j-1_1}\right) \\
& -\gamma\left(2\, z_{j_0}^3 - z_{j+1_0}^3 - z_{j-1_0}^3\right)
\end{aligned}
\tag{10}
$$

We assume a traveling wave solution to solve the ε^0 equation (8). Let

$$
z_{j_0} = y_{j_0} + \bar{y}_{j_0} = A e^{i(kx_j - \omega_0 T_0)} + \bar{A} e^{-i(kx_j - \omega_0 T_0)} \tag{11}
$$

where $y_{j_0} = A e^{i(kx_j - \omega_0 T_0)}$. Then $y_{j\pm 1_0} = A e^{i(kx_{j\pm 1} - \omega_0 T_0)}$. We also assume $x_{j\pm 1} = x_j \pm h$. Plugging in $y_{j\pm 1_0} = e^{\pm ikh} A e^{i(kx_j - \omega_0 T_0)} = e^{\pm ikh} y_{j_0}$, into equation (8) we get

$$
\omega_0^2 = 2\alpha(1 - \cos kh) \tag{12}
$$

Hence, letting $A = \frac{1}{2} a e^{-ib}$,

$$
z_{j_0} = y_{j_0} + \bar{y}_{j_0} = \frac{1}{2} a e^{i(kx_j - \omega_0 T_0 - b)} + c.c. \tag{13}
$$

The solution to ε^0 equation can be used in equation (9) to find the secular terms. The solvability condition is $-2D_0D_1 z_{j_0} = 2(i\omega_0) A' e^{i(kx_j - \omega_0 T_0)} + c.c.$, resulting in $A' = 0$, where $()' = \frac{\partial}{\partial T_1}$. Hence $a' = 0$ and $b' = 0$, such that

$$
\begin{aligned}
a &= a(T_2) \\
b &= b(T_2)
\end{aligned}
\tag{14}
$$

Removing the secular term, we write the ε^1 equation as

$$
\begin{aligned}
&D_0^2 z_{j_1} + \alpha\left(2\, z_{j_1} - z_{j+1_1} - z_{j-1_1}\right) \\
&= -\beta\left(2\, z_{j_0}^2 - z_{j+1_0}^2 - z_{j-1_0}^2\right) \\
&= -\beta\left(2 - e^{2ikh} - e^{-2ikh}\right)\left(\frac{1}{2} a e^{-ib}\right)^2 e^{2i(kx_j - \omega_0 T_0)} + c.c. \\
&= -\frac{\beta a^2}{2}(1 - \cos 2kh) e^{2i(kx_j - \omega_0 T_0 - b)} + c.c.
\end{aligned}
\tag{15}
$$

Assuming the particular solution to the above equation to be of the form,

$$
z_{j_1} = A_1 e^{2i(kx_j - \omega_0 T_0 - b)} + c.c. \tag{16}
$$

Plugging this into the ε^1 equation and balancing the coefficients of $e^{2i(kx_j - \omega_0 T_0 - b)}$ leads to

$$
A_1 = \frac{\beta a^2 \sin^2 2kh}{4\left(\omega_0^2 - \alpha \sin^2 kh\right)} \tag{17}
$$

The solution to ε^1 equation is therefore

$$
z_{j_1} = \frac{\beta a^2 \sin^2 kh}{4\left(\omega_0^2 - \alpha \sin^2 kh\right)} e^{2i(kx_j - \omega_0 T_0 - b)} + c.c. \tag{18}
$$

We will now examine the ε^2 equation in order to solve for a and b. We note that z_{j_0} and z_{j_1} are independent of T_1. Therefore $-2D_0D_1 z_{j_1}$ and $D_1^2 z_{j_0}$ vanish. Plugging z_{j0} and z_{j1} into the equation (10), we obtain

$$
\begin{aligned}
&D_0^2 z_{j_2} + \alpha\left(2\, z_{j_2} - z_{j+1_2} - z_{j-1_2}\right) \\
&= -\left[(a' - aib')(-i\omega_0) e^{i(kx_j - \omega_0 T_0 - b)} + c.c.\right] \\
&-\beta \frac{\beta a^3 \sin^2 kh}{8\left(\omega_0^2 - \alpha \sin^2 kh\right)}\left[(2 - e^{3ikh} - e^{-3ikh}) e^{3i(kx_j - \omega_0 T_0 - b)}\right. \\
&\qquad\qquad \left. + (2 - e^{ikh} - e^{-ikh}) e^{i(kx_j - \omega_0 T_0 - b)} + c.c.\right] \\
&-\gamma \frac{a^3}{8}\left[(2 - e^{3ikh} - e^{-3ikh}) e^{3i(kx_j - \omega_0 T_0 - b)}\right. \\
&\qquad\qquad \left. + 3(2 - e^{ikh} - e^{-ikh}) e^{i(kx_j - \omega_0 T_0 - b)} + c.c.\right]
\end{aligned}
\tag{19}
$$

where, $a' = \frac{\partial a}{\partial T_2}$, and $b' = \frac{\partial b}{\partial T_2}$. The secular terms from the above equation are the coefficients of $e^{i(kx_j - \omega_0 T_0)}$. Eliminating the secular term results in

$$(i\omega_0 a' + \omega_0 a b') = \left[\frac{3\gamma}{4} + \frac{\beta^2 \sin^2 kh}{2\left(\omega_0^2 - \alpha \sin^2 kh\right)}\right](1-\cos kh)a^3 \tag{20}$$

Equating the real and imaginary parts, the solvability condition can be written as

$$\begin{aligned} &\text{Im:} \quad a' = 0 \\ &\text{Re:} \quad \omega_0 a b' = \left[\frac{3\gamma}{4} + \frac{\beta^2 \sin^2 kh}{2\left(\omega_0^2 - \alpha \sin^2 kh\right)}\right](1-\cos kh)a^3 \end{aligned} \tag{21}$$

Using ω_0 from equation (12), in equation (21), we get

$$\begin{aligned} &\text{Im:} \quad a' = 0 \\ &\text{Re:} \quad b' = \left[\frac{3\gamma}{4} + \frac{\beta^2(1+\cos kh)}{2\alpha(1-\cos kh)}\right]\frac{\omega_0}{2\alpha}a^2 \end{aligned} \tag{22}$$

Solving the equation (22), we get

$$\begin{aligned} a &= a_0 \\ b &= \left[\frac{3\gamma}{4} + \frac{\beta^2(1+\cos kh)}{2\alpha(1-\cos kh)}\right]\frac{\omega_0}{2\alpha}a_0^2 T_2 + b_c \end{aligned} \tag{23}$$

We can neglect integration constant b_c without loss of generality. Also we note that $T_2 = \varepsilon^2 T_0$. Hence the slowly varying amplitude (a) and phase (b) becomes,

$$\begin{aligned} a &= a_0 \\ b &= \left[\frac{3\gamma}{4} + \frac{\beta^2(1+\cos kh)}{2\alpha(1-\cos kh)}\right]\frac{\omega_0}{2\alpha}a_0^2 \varepsilon^2 T_0 \end{aligned} \tag{24}$$

Therefore combining equation (11) with $A = \frac{1}{2}ae^{-ib}$, the frequency ω can be written as

$$\begin{aligned} \omega &= \omega_0 + \frac{b}{T_0} \\ &= \omega_0\left[1 + \frac{\varepsilon^2 a_0^2}{2\alpha}\left(\frac{3\gamma}{4} + \frac{\beta^2(1+\cos kh)}{2\alpha(1-\cos kh)}\right)\right] \end{aligned} \tag{25}$$

3.2 Frequency Expression in Displacement Coordinates

The above solution in equation (25) is obtained by solving the EOM in strain coordinates $z_j = u_{j+1} - u_j$, where u_j is in the displacement coordinates. We now interprete the solution in displacement coordinates. Let the solution in u coordinates be $u_j = De^{i(kx_j - \omega t)} + c.c.$ and $u_{j+1} = De^{i(kx_{j+1} - \omega t)} + c.c. = De^{ikh}e^{i(kx_j - \omega t)} + c.c.$. Therefore

$$z_j = D(e^{ikh} - 1)e^{i(kx_j - \omega t)} + c.c. = Ae^{i(kx_j - \omega t)} + c.c. \tag{26}$$

Letting $D = \frac{1}{2}d_0 e^{-i\theta}$, we get the relationship between the amplitudes in displacement and strain coordinates as

$$\begin{aligned} A &= \frac{1}{2}d_0 e^{-i\theta}(e^{ikh} - 1) = \frac{1}{2}d_0 e^{-i\theta}(\rho e^{i\phi}) \\ \text{or} \quad \frac{1}{2}a_0 e^{-ib} &= \frac{1}{2}\rho d_0 e^{-i(\theta - \phi)} \end{aligned} \tag{27}$$

where, with help from equation (12),

$$\begin{aligned} &\rho = \sqrt{(\cos kh - 1)^2 + \sin^2 kh} = \sqrt{2(1-\cos kh)} = \sqrt{\frac{\omega_0^2}{\alpha}} \\ &\tan\phi = \frac{\sin kh}{\cos kh - 1} = -\cot\frac{kh}{2} = \tan\left(\frac{\pi}{2} + \frac{kh}{2}\right) \\ &a_0 = \rho d_0 \end{aligned} \tag{28}$$

Hence the amplitude and phase in strain coordinates are related to the amplitude and phase in displacement coordinates by

$$\begin{aligned} a_0^2 &= \frac{\omega_0^2}{\omega_n^2}d_0^2 \\ \tan\phi &= \tan\left(\frac{\pi}{2} + \frac{kh}{2}\right) \end{aligned} \tag{29}$$

where $\omega_n^2 = \alpha$. Therefore the frequency in the displacement coordinate system can be written as

$$\omega(k, d_0) = \omega_0\left[1 + \varepsilon^2\left\{\frac{3\gamma}{4} + \frac{\beta^2}{2\alpha}\left(\frac{1+\cos kh}{1-\cos kh}\right)\right\}\frac{\omega_0^2 d_0^2}{2\alpha^2}\right] \tag{30}$$

Also note that, in the above dispersion relationship, ω_0 is a function of the wave number k.

3.3 Comparison in Continuum Limit

To check the correlation between the coordinates, we consider a continuum. The displacement at any location x in the continuum is assumed to be of the following form

$$u(x_j) = De^{i(kx_j - \omega t)} \tag{31}$$

The strain can then be found by taking the partial derivative of the displacement with respect to position x to get

$$z(x_j, t) = \frac{\partial u(x_j)}{\partial x_j} = D(ik)e^{i(kx_j - \omega t)} = Dke^{i\frac{\pi}{2}}e^{i(kx_j - \omega t)} \tag{32}$$

To obtain the continuum limit in our MMS solution, we first represent the amplitude and phase of our solution (strain) in displacement coordinate system and then take the limit as $h \to 0$. Making use of

$$\lim_{h\to 0} \frac{sin(kh)}{h} = k \tag{33}$$

and the equations (26) - (28) the strain can be found as

$$\begin{aligned} z(x_j,t) &= \lim_{h\to 0} \frac{z_j(x_j,t)}{h} = \lim_{h\to 0} A\frac{1}{h}e^{i(kx_j-\omega t)} \\ &= \lim_{h\to 0} D\frac{1}{h}(e^{ikh}-1)e^{i(kx_j-\omega t)} = \lim_{h\to 0} D\rho\frac{1}{h}e^{i\phi}e^{i(kx_j-\omega t)} \\ &= \lim_{h\to 0} D\frac{2sin\left(\frac{kh}{2}\right)}{h}e^{i(\frac{\pi}{2}+\frac{kh}{2})}e^{i(kx_j-\omega t)} = Dke^{i\frac{\pi}{2}}e^{i(kx_j-\omega t)} \end{aligned} \tag{34}$$

Hence the strain from both the equations (32) and (34) are identical and confirms the validity of the coordinate transformations between the strain and displacement coordinates.

4 Interpretations of Results

From the amplitude and phase we have obtained from second order MMS analysis of traveling wave solutions, we find interesting results in the dispersion diagram as well as in the relationship between the group and phase velocities with respect to wave number (k).

For $\alpha = 3$, $d_0 = 1$, $h = 1$, we plot the dispersion diagram from equation (30) for $\beta = 0$, and $\beta = -4$. As we vary γ as -1, 0 and 1, we see that due to the quadratic effect (for $\beta = -4$) the frequency is higher in the lower wave number region as compared to the $\beta = 0$ case as seen in the Figure 3.

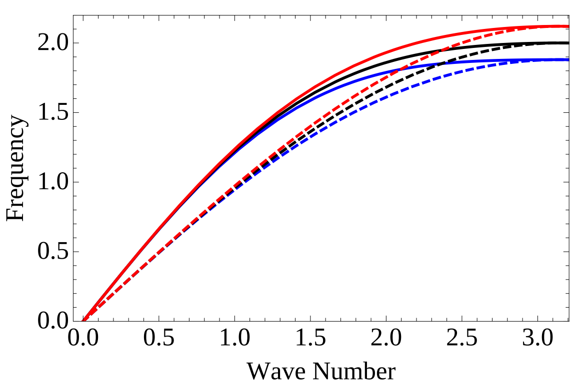

FIGURE 3: The dispersion diagram. x-axis represents the wave number (k) and y-axis represents the frequency ($\omega(d_0,k)$). Solid and dashed curves correspond to ($\alpha > 0$, $\beta < 0$), and ($\alpha > 0$, $\beta = 0$) respectively. $\gamma = -1$ (blue), 0 (black), 1 (red).

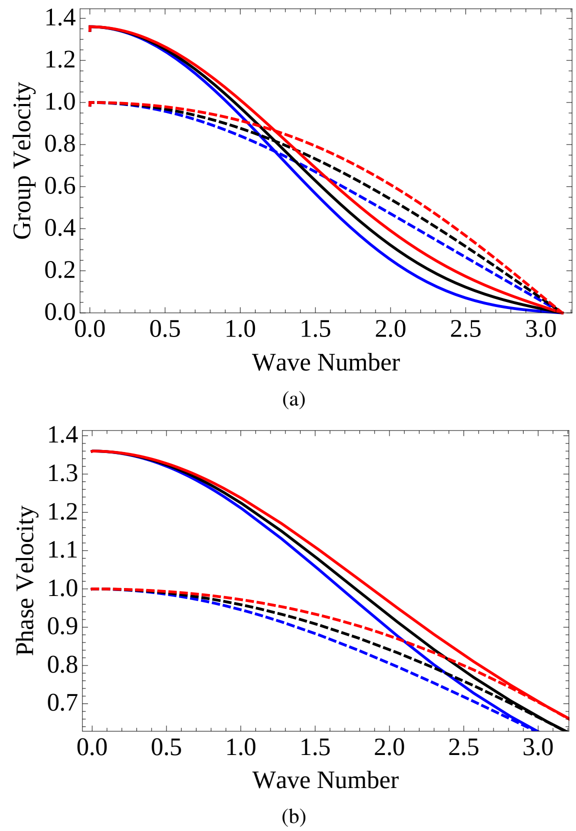

FIGURE 4: (a) Group velocity ($c(d_0,k)$) and (b) phase velocity ($v_g(d_0,k)$) w.r.t. the wave number (k). Solid and dashed curves correspond to ($\alpha > 0$, $\beta \neq 0$), and ($\alpha > 0$, $\beta = 0$) respectively.

The phase velocity ($c(d_0,k)$) and group velocity ($v_g(d_0,k)$) can be found from the following relation between the frequency and wave number:

$$\begin{aligned} c\ (k,d_0) &= \frac{\omega(k,d_0)}{k} \\ v_g\ (k,d_0) &= \frac{d\omega(k,d_0)}{dk} \end{aligned} \tag{35}$$

based on equation (30).

We see from the Figure 4, that due to the quadratic effect the group and phase velocities, plotted by applying equations (35) to equation (30) are much higher for smaller wave numbers as compared to the $\beta = 0$ case. For fixed wave number $k = 0.4\pi$, as we change amplitude from 0 to 1, we observe that the phase velocity is much higher with quadratic terms, whereas the group velocity does not change significantly as shown in Figure 5. Considering the scales of the plots, the amplitude effect (Figure 5(a)) on group velocity is small.

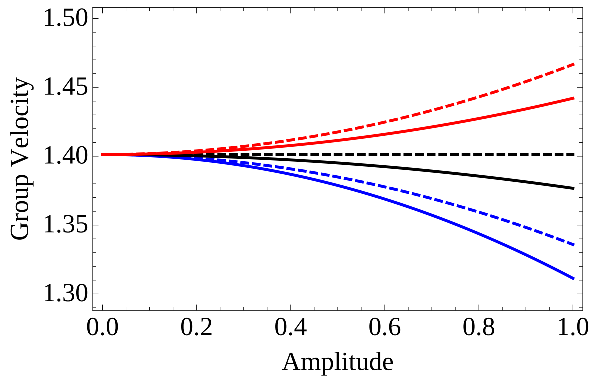

(a)

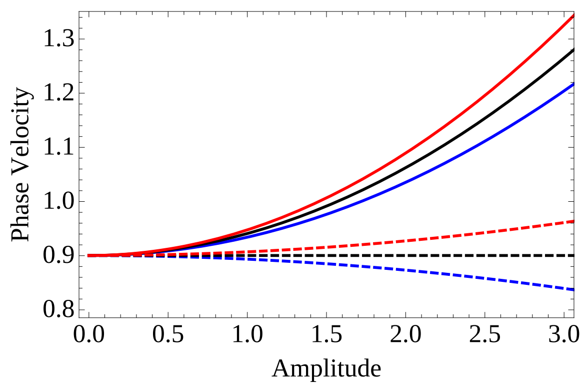

(b)

FIGURE 5: (a) Group velocity ($c(d_0,k)$) and (b) phase velocity ($v_g(d_0,k)$) w.r.t. the amplitude (d_0) for a particular wave number $k = 0.4\pi$. Solid and dashed curves correspond to ($\alpha > 0$, $\beta \neq 0$), and ($\alpha > 0$, $\beta = 0$) respectively.

5 Conclusions and Outlook

In this paper we have presented a detailed study of traveling wave behavior in an infinite periodic chain of snap-through elements for low-amplitude oscillations. We adapted a second-order multiple-scales analysis to accommodate traveling waves. This analysis uncovered dispersion relationships, and the effects of quadratic and cubic nonlinearities, as well as wave amplitude. The quadratic nonlinearities have a significant effect on the dispersion characteristics because we have considered small amplitude oscillations where the system does not exhibit twinkling. A comparison between the quadratic (with nonzero cubic terms) and cubic (no quadratic terms) cases shows that the quadratic terms lead to much higher phase and group velocities for lower wave numbers. At higher wave numbers, however, the group velocities for the quadratic case are much lower as compared to the cubic case. The second-order perturbation analysis for the traveling wave study showed interesting behavior of the system in presence of quadratic nonlinearity. Future work will include a wave-wave interactions, and possible large amplitude waves.

ACKNOWLEDGMENT

This material is based upon work supported by the National Science Foundation under Grant No. CMMI-1030377. Any opinions, findings, and conclusions or recommendations expressed in this material are those of the authors and do not necessarily reflect the views of the National Science Foundation.

REFERENCES

[1] Page, J., Sukhovich, A., Yang, S., Cowan, M., van der Bi-est, F., Tourin, A., Fink, M., Liu, Z., Chan, C., and Sheng, P., 2004. “Phononic crystals”. *Solid State Physics,* ***241***(15), pp. 3454–3462.

[2] Bertoldi, K., and Boyce, M., 2008. “Mechanically triggered transformations of phononic band gap elastomeric structures”. *Physical Review B,* ***77***(052105).

[3] Jang, J. H., Ullal, C. K. U., Gorishnyy, T., Tsukruk, V. V., and Thomas, E. L., 2006. “Mechanically tunable three-dimensional elastomeric network/air structures via interference lithography”. *Nano Letters,* ***6***(4), pp. 740–743.

[4] Liang, B., Yuan, B., and Cheng, J. C., 2009. “Acoustic diode: Rectification of acoustic energy flux in one-dimensional systems”. *Physical Review Letters,* ***13***, p. 104301.

[5] Olsson, R. H. I., El-Kady, I. F., Su, M. F., Tuck, M. R., and Fleming, J. G., 2008. “Microfabricated vhf acoustic crystals and waveguides”. *Sensors and Actuators A: Physical,* ***20***(1), pp. 87–93.

[6] Olsson, R. H. I., and El-Kady, I., 2009. “Microfabricated phononic crystal devices and applications”. *Measurement Science and Technology,* ***20***(1), p. 012002.

[7] Sigmund, O., and Jensen, J. S., 2003. “Systematic design of phononic band-gap materials and structures by topology optimization”. *Philosphical Transactions of the Royal Society A: Mathematical, Physical and Engineering Sciences,* ***361***(1806), pp. 1001–1019.

[8] Yun, Y., Miao, G. Q., Zhang, P., Huang, K., and Wei, R. J., 2005. “Nonlinear acoustic wave propagating in one-dimensional layered system”. *Physics Letters A,* ***343***(5), pp. 351–358.

[9] Marathe, A., and Chatterjee, A., 2005. “Wave attenuation in nonlinear periodic structures using harmonic balance and multiple scales.”. *Journal of Sound and Vibration,* ***289***(4-5), pp. 871–888.

[10] Narisetti, R. K., Leamy, M. J., and Ruzzene, M., 2010. “A perturbation approach for predicting wave propagation in one-dimensional nonlinear periodic structures”. *ASME Journal of Vibration and Acoustics,* ***132***(3), p. 031001.

[11] Narisetti, R. K., Ruzzene, M., and Leamy, M. J., 2011. "A perturbation approach for analyzing dispersion and group velocities in two-dimensional nonlinear periodic lattices". *ASME Journal of Vibration and Acoustic,* ***133***(6), p. 061020.

[12] Nayfeh, A. H., and Rice, M. H., 1972. "On the propagation of disturbances in a semi-infinite one-dimensional lattice". *American Journal of Physics,* ***40***(3), pp. 469–470.

[13] Daraio, C., Nesterenko, V. F., Herbold, E. B., and Jin, S., 2005. "Strongly nonlinear waves in a chain of teflon beads". *Physical Review E,* ***72***(1), p. 016603.

[14] Peyrard, M., and Kruskal, M. D., 1984. "Kink dynamics in the highly discrete sine-gordon system". *Physica D,* ***14***(1), pp. 88–102.

[15] Vakakis, A. F., and King, M. E., 1995. "Nonlinear wave transmission in a monocoupled elastic periodic system". *Journal of Acoustical Society of America,* ***98***(3), pp. 1534–1546.

[16] Vakakis, A. F., and King, M. E., 1998. "Resonant oscillations of a weakly coupled, nonlinear layered system". *Acta Mechanica,* ***128***(1), pp. 59–80.

[17] Asfar, O. R., and Nayfeh, A. H., 1983. "The application of the method of multiple scales to wave propagation in periodic structures". *Society of Industrial and Mathematics Review,* ***25***(4), pp. 455–480.

[18] Chakraborty, G., and Mallik, A. K., 2001. "Dynamics of a weakly nonlinear periodic chain". *International Journal of Non-linear Mechanics,* ***36***(2), pp. 375–389.

[19] Rushchitsky, J. J., and Saveleva, E. V., 2006. "On the interaction of cubically nonlinear transverse plane waves in an elastic material". *International Applied Mechanics,* ***42***(6), pp. 661–668.

[20] Rothos, V. M., and Vakakis, A. F., 2009. "Dynamic interactions of traveling waves propagating in a linear chain with an local essentially nonlinear attachment". *Wave Motion,* ***46***(3), pp. 174–188.

[21] I., H. M., Hulbert, G., and Scott, R., 2002. "Tailoring of wave propagation characteristics in periodic structures with multilayer unit cells". *Proceedings of 17th American Society of Composites Technical Conference*.

[22] I., H. M., Hamza, K., Hulbert, G., and Saitou, K., 2007. "Optimal synthesis of 2d phononic crystals for broadband frequency isolation". *Waves Random Complex Media,* ***17***(4).

[23] Diaz, A., Haddow, A., and Ma, L., 2005. "Design of band-gap grid structures". *Structural and Multidisciplinary Optimization,* ***29***(6), pp. 418–431.

[24] Manktelow, K., Leamy, M. J., and Ruzzene, M., 2011. "Multiple scales analysis of wave–wave interactions in a cubically nonlinear monoatomic chain". *Nonlinear Dynamics,* ***63***, pp. 193–203.